A Journal of the Gesellschaft Deutscher Chemiker

Angewandte International Edition

GDCh

Chemie

www.angewandte.org

Accepted Article

Title: Strong N−X···O−N Halogen Bonds: Comprehensive Study on N-Halosaccharin Pyridine N-oxide Complexes

Authors: Kari Rissanen, Rakesh Puttreddy, Mikko Rautiainen, and Toni Mäkelä

To be cited as: *Angew. Chem. Int. Ed.* 10.1002/anie.201909759
Angew. Chem. 10.1002/ange.201909759

Link to VoR: http://dx.doi.org/10.1002/anie.201909759
http://dx.doi.org/10.1002/ange.201909759

WILEY-VCH

10.1002/anie.201909759

WILEY-VCH

RESEARCH ARTICLE

Strong N−X··O−N Halogen Bonds: Comprehensive Study on N-Halosaccharin Pyridine *N*-oxide Complexes

Rakesh Puttreddy,*[a] J. Mikko Rautiainen,[a] Toni Mäkelä,[a] Kari Rissanen*[a]

Dedicated to Professor Dr. Dieter Enders

Abstract: A detailed study of the strong N−X···$^{-}$O−N^{+} (X = I, Br) halogen bonding interactions in solution and in the solid-state reports 2×27 donor×acceptor complexes of *N*-halosaccharins and pyridine *N*-oxides (PyNO). Density Functional Theory (DFT) calculations were used to investigate the X···O halogen bond (XB) interaction energies in 54 complexes. The XB interaction energies were found to vary from –47.5 to –120.3 kJ mol^{-1}, with the strongest N−I···$^{-}$O−N^{+} XBs approaching those of 3-*center*-4-*electron* [N–I–N]$^{+}$ halogen-bonded systems (~160 kJ mol^{-1}). Using a subset of 32 complexes, stabilized only through N−X···$^{-}$O−N^{+} XB interactions, a simplified, computationally fast, electrostatic model to predict the X···O bond energies, was developed. Energies predicted by this simple model and much higher-level theory DFT calculations agree excellently, illustrating the usefulness of the simplified electrostatic model. In solution, the ^{1}H NMR association constants (K_{XB}) determined in $CDCl_3$ and acetone-d_6 vary from 2.0 x10^{0} to >10^{8} M^{-1} following accurately the calculated σ-hole nature on the donor halogen. The donor×acceptor complexation enthalpies calculated in $CHCl_3$ using polarized continuum model very between –38.4 and –77.5 kJ mol^{-1} and correlate well with the pK_{XB} values determined by ^{1}H NMR in $CDCl_3$ indicating the formation of strong and robust 1:1 XB complexes in solution. In X-ray crystal structures, the *N*-iodosaccharin-PyNO complexes manifest short normalized interaction ratios (R_{XB}) between 0.65 – 0.67 for the N−I···$^{-}$O−N^{+} halogen bond.

Introduction

Halogen bonding,[1] the attractive non-covalent interaction between electrophilic region of the halogen atom and an electron donor, has been extensively studied in supramolecular chemistry as an alternative to hydrogen bond (HB).[2] The high directional nature and tunability of halogen bonding interaction has allowed to design catalysts,[3–5] receptors for anion recognition,[6] materials,[7–12] liquid crystals,[13,14] and gels.[15–17]. In principle, any Lewis base can act as a halogen bond (XB) acceptor,[1] yet due to easy access of N-heterocycles, the nitrogen atom has been predominantly exploited as the XB acceptor.[18] The effect of halogen in perfluorohalo -alkyl and -aromatic donors on the XB strengths formed with N-heterocycles have been studied by using computational methods,[19] X-ray crystallography,[20] and solution NMR.[21–24] The influence of electron density modulation of N-heterocycles nitrogen atom on the XB strengths with non-fluorinated aromatic XB donors is also well-documented in the literature.[13,25–31] Halonium ions, X^{+}, form very strong XBs with N-heterocycles,[32–40] generating [N–X–N]$^{+}$ type complexes with the smallest R_{XB} values reported for [X–N]$^{+}$ distances in solid-state X-ray crystal structures (R_{XB} = 0.61-0.66) [See Table S1].

In our quest for strong yet alternative XBs, we have reported a simple approach that utilizes N-iodosuccinimide and N-bromosuccinimide as the XB donors and hexamethylenetetramine as the XB acceptor to prepare (OC)$_2$N–I···N and (OC)$_2$N–Br···N type strong XBs.[41,42] Similarly Fourmigué *et al*. have shown using N-iodosaccharin (NISac) and highly nucleophilic 4-*N*,*N*-dimethylaminipyridine (DMAP) as the XB acceptor, that the N–I bond of the N-haloimide can be dissociated forming an iodo-pyridinium cation and N-saccharinate anion, *viz*. forming a salt.[43,44] While strong XBs with N-heterocycles are common, the development of (strong) halogen bonds using other Lewis bases *e.g*. (*N*-oxide) oxygen, has remained largely unexplored.[45–61]

The synthesis of [N–I–N]$^{+}$ complexes by Ag(I) cation exchange reaction has enabled construction of complex halonium ion-based supramolecular structures.[62–64] The results by Erdélyi *et al*. provided useful information on the strength and geometry of the [N−X−N]$^{+}$ XBs.[65–71] In [bis(pyridine)iodine]$^{+}$ complexes, computational studies revealed that the substituents at the *para*-position to the pyridine N-atom influence the XB stabilization energies, reflected by their [N−I^{+}] bond lengths.[70] However, the cation exchange process and the stabilization of I^{+} ion by two identical N-heterocycles has prevented the determination of solution association constants for [N–I–N]$^{+}$ complexes. In our previous study, we have shown that the strong and tuneable N−X···$^{-}$O−N^{+} halogen bonds are formed by using two heteronuclear aromatic components, *viz*. N-haloimides as donors and pyridine *N*-oxides (PyNOs) as acceptors.[72] Unlike the [N–X–N]$^{+}$ synthesis,[67,70,71] this approach does not require dry solvent conditions, either for solution NMR studies or crystallization experiments. Solution studies of the 1:1 N-haloimide:PyNO complexes showed that high binding constants manifested shorter X···O halogen bond distances with R_{XB} values < 0.70.[69]

In the present study, we investigate the nature of the N−X···$^{-}$O−N^{+} interactions and their strength dependence by using 2×27 donor×acceptor complexes [Fig.1]. Our strategy involves introducing methyl, methoxy and phenyl substituents at *ortho*-, *meta*- and *para*-positions to $^{+}$N−O^{-} group in PyNOs, and combining them with N-halosaccharins to evaluate N−X···$^{-}$O−N^{+} XB interaction strengths. Three techniques were used to elucidate the results: (a) computational studies, (b) solution NMR and (c) single-crystal X-ray diffraction analysis. The N-halosaccharins and most of the PyNOs utilized in the current study are commercially available. A few of the *N*-oxides were synthesized

[a] Dr. Rakesh Puttreddy, Dr. J. Mikko Rautiainen, Dr. Toni Mäkelä, Prof. Dr. Kari Rissanen
University of Jyvaskyla, Department of chemistry, *P.O.* BOX 35, FI-40014, Jyväskylä, Finland
E-mail: rakesh.r.puttreddy@jyu.fi, kari.t.rissanen@jyu.fi

Supporting information for this article is given via a link at the end of the document.

10.1002/anie.201909759

by the oxidation of their corresponding pyridines using well-established synthesis methods.[73]

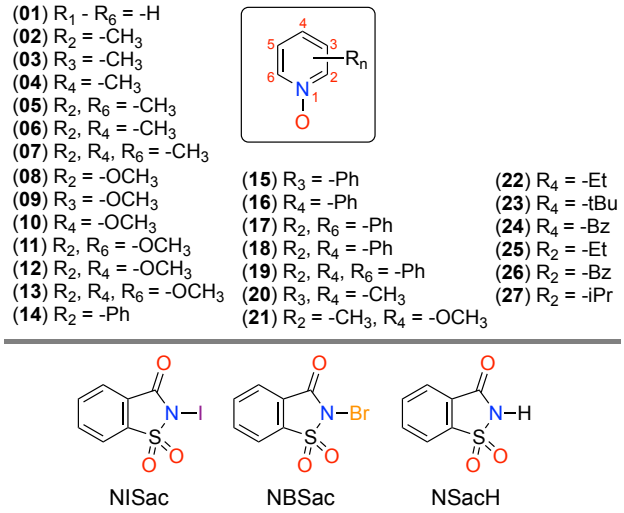

Figure 1. List of components: pyridine *N*-oxides (**1** - **27**) as XB acceptors (above), and N-halosaccharins as XB donors (below): N-iodosaccharin (NISac), N-bromosaccharin (NBSac) and HB donor saccharin (NSacH).

Results and Discussion

Computational Studies: Simplified Electrostatic Model (ΔE_{model}) for N−X···$^{-}$O−N^{+} Halogen Bonds

To elucidate N−X···$^{-}$O−N^{+} interactions, we employ the electrostatic/polarization model promoted by Politzer *et al*. that allows the prediction of interaction strengths by using only the inherent properties of the donors and acceptors.[74–76] The computational results are correlated with experimental association constants (K_{XB}) and X-ray crystal structure bond parameters. We have used two DFT methods, a widely employed hybrid-DFT method PBE0-D3/def2-TZVP and a computationally more demanding combination of a range-separated functional and augmented triple-ζ quality basis set ωB97X-D/aug-cc-pVTZ(PP).[77] The latter method has been recommended in a large benchmark study for calculating accurate XB energies,[78] but for the purposes of this study both methods gave results of comparable quality. The PBE0-D3/def2-TZVP results are used for the discussions here, while the ωB97X-D/aug-cc-pVTZ(PP) results are included in the SI.

The interaction energies (ΔE_{int}) of 54 optimized XB complexes were correlated with the calculated X···O distances but showed relatively low R^2 values of 0.582 and 0.463, for X = Br and I, respectively. A closer review of the optimized structures revealed that 11 complexes from each N-I/BSac-**Z** series (where **Z** is an XB acceptor) deviate from the ΔE_{int} vs X···O linear relation and form a set on their own [Fig. 2a, Fig. S2]. These 22 1:1 complexes manifest additional non-covalent interactions such as H-bonding and lone pair-π interactions that could subtly affect the N−X···$^{-}$O−N^{+} interactions [for examples, see SI, Fig. S3]. By removing these "biasing" 22 structures from the further analyses, the linear correlation improves significantly to R^2 = 0.913 for NBSac-**Z** and 0.901 for NISac-**Z** complexes. This correlation between ΔE_{int} and X···O distances contrasts with quadratic polynomial dependence reported by Zou *et al*.[79] In the Zou study, the ΔE_{int} vs interatomic distances are compared over a wide distance range (2.10 – 3.40 Å) for R–X···NH_3 (X = Cl, Br, I) type XBs. Non-linear correlations are to be expected when interactions are examined over wide ranges as interatomic interactions are known to follow Morse potential[80] type of behaviour. However, for narrow range of interatomic N−X···$^{-}$O−N^{+} interactions (2.34 – 2.46 Å) a simple linear dependence seems to sufficiently describe the relation between ΔE_{int} and XB distances. The ΔE_{int} vs R_{XB} for I···O and Br···O bond distances in 32 computed structures, that are unbiased by additional interactions, have a combined correlation coefficient, R^2 = 0.954 [SI, Fig. S6]. The results suggest that the correlations, ΔE_{int} vs X···O and ΔE_{int} vs R_{XB}, could be used to differentiate energies of N−X···$^{-}$O−N^{+} interactions from 1:1 donor:acceptor complexes stabilized by both halogen bonding and H-bonding.

The influence of the additional interactions on halogen bond ΔE_{int} values can be qualitatively estimated by the optimization of *e.g.* NISac-**15** and NBSac-**15** to higher energy conformations obtained by the rotation of 3-phenyl substituent around the C−C single bond away from the donor -SO_2 group to disrupt the C−H···O_2S H-bonding interaction [SI, Fig. S4]. The ΔE_{int} of the global minimum structures of NISac-**15** [–84.1 kJ mol^{-1}] and NBSac-**15** [–59.5 kJ mol^{-1}] are, respectively, 11.5 and 10.5 kJ mol^{-1}, stronger than the ΔE_{int} of structures where the C−H···O_2S interactions are not present. The influence of the acceptor conformations on XB energies is in line with the pyridyl conformational studies reported for [N−X−N]$^{+}$ XBs,[71] which supports the role of H-bonding in stabilizing some of the XB complexes. The calculated ΔE_{int} vary, from –84.3 to –120.3 kJ mol^{-1} for NISac-**Z**, and from –47.5 to –81.5 kJ mol^{-1} for NBSac-**Z** complexes. The largest ΔE_{int} in both series for NISac-**13** (–120.3 kJ mol^{-1}) and NBSac-**12** (–81.5 kJ mol^{-1}) are, weaker than the corresponding 3-center-4-electron (3*c*4*e*) XBs, [N−I−N]$^{+}$ (–159.2 kJ mol^{-1})[65] and [N-Br-N]$^{+}$ (–151.0 kJ mol^{-1}),[65] respectively, yet stronger than the other reported similar XBs *e.g.* I−I···$^{-}$O−N^{+} (–42.0 kJ mol^{-1}),[46] CF_3−I···$^{-}$O−N^{+} (–33.7 kJ mol^{-1}),[55] NISac···N_{py} (**Py** = pyridine; –61.4 kJ mol^{-1}),[81] NBSac···N_{py} (–43.5 kJ mol^{-1}),[81] NBS···N_{Py} (–38.6 kJ mol^{-1}),[81] and $C_6F_4Br_2$···N_{bpe} (**bpe** = 1,2-bis(4-pyridyl)ethylene, –14.5 kJ mol^{-1})[82] complexes. This comparison evidence the strong binding that can be achieved by N−X···$^{-}$O−N^{+} (X = Br, I) XBs.

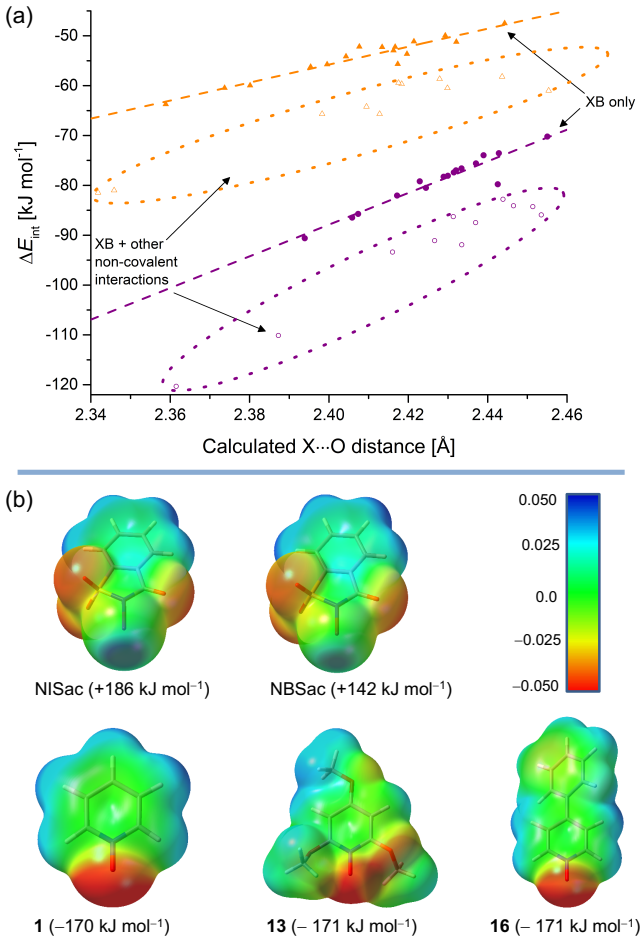

Figure 2. (a) Correlation between X···O distances vs ΔE_{int} calculated at PBE0-D3/def2-TZVP level of theory for NISac-**Z** (purple dots) and NBSac-**Z** (orange triangles). Open triangles and dots are XB complexes with additional intermolecular interactions. (b) Computed electrostatic potentials projected on the 0.001 au electron density surfaces of XB donors with $V_{S,max}$ values, (top) NISac and NBSac and selected PyNOs (**1**, **13**, and **16**) with $V_{S,min}$ values.

To test the applicability of the simplified electrostatic model for describing N−X···$^{-}$O−N^{+} (X = Br, I) XBs, energies (ΔE_{model}) obtained from the double regression of the local positive maxima of electrostatic surface potential, $V_{S,max}$ of donor molecules and the local negative maxima of electrostatic surface potential, $V_{S,min}$ of acceptor molecules were correlated with ΔE_{int} values of 32 XB complexes [Fig. 2b].[83–86] A reasonably good correlation, R^2 = 0.896, was obtained but the data points formed two distinct groups, matching the donor σ-hole strengths [SI, Fig. S8]. The two sets of data points imply that the influence of the acceptor to the XB interaction strengths is not properly accounted by $V_{S,min}$ alone. We assumed that the poor correlation could be related to the difference between the location of the $V_{S,min}$ on the O-atoms parallel to N−O bonds and the XB formation sites, which are nearly orthogonal to N−O bonds as shown in Fig. 3. The bonding situation contrasts with the pyridine N-acceptor based XB complexes,[85] where the $V_{S,min}$ of the nitrogen, *e.g.* pyridine (**Py**), parallels with the X···N halogen bond as depicted in Fig. 3. To account for the spatial difference, the use of electrostatic surface potential value V_S in the direction of the halogen bond would be more appropriate. However, since the location of X···O interaction and thus the position of V_S is not known prior to XB complexation, we opted to use oxygen atomic charges (Q_{oxygen}) as average measures of the influence the oxygen electron density has on the XB interaction strengths. This approach improved the correlation significantly to R^2 = 0.976 [SI, Fig. S10].

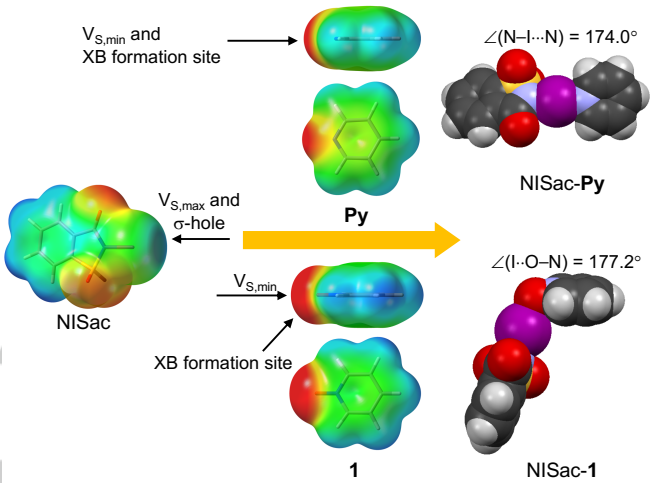

Figure 3. Computed electrostatic potentials projected on the 0.001 au electron density surfaces of NISac, Pyridine (**Py**) and **1**, and crystal structures of NISac-**Py**[87] and NISac-**1**.

To factor in the known influence of the mutual polarization of donor and acceptor components on XB strengths [75,76] to the bonding model, minima of average local ionization energies, $I_{S,min}$ (eV),[89,90] of O-atom as the inverse measure of polarizability was included in the ΔE_{model} as shown by the equation in Fig. 4.[86] Furthermore, following Coulomb's law, the products of Q_{oxygen} and $V_{S,max}$ are used in the final correlation of ΔE_{model} against ΔE_{int}, which leads to small improvement in the correlation, R^2 = 0.983 [Fig. 4]. Further development of the model by including $1/I_{S,min}$ of halogen to describe its polarizability did not improve the fit further [SI, Figs. S14 and S15]. With the final model [Fig. 4] the root mean square (RMS) deviation between the ΔE_{model} and the energies from the PBE0-D3/def2-TZVP calculations is 1.7 kJ mol^{-1} and the maximum difference is 3.1 kJ mol^{-1}. By comparison, using the ωB97X-D/aug-cc-pVTZ(PP) method, ΔE_{model} vs ΔE_{int} resulted in only slightly better correlation with R^2 = 0.994, smaller RMS deviation of energies 1.0 kJ mol^{-1}, and maximum energy difference of 2.2 kJ mol^{-1}.

Table 1. ^{1}H NMR Association constants (K_{XB}, M^{-1}, 298.0K) for NISac-**Z** and NBSac-**Z** (**Z** = **1**-**27**) complexes in $CDCl_3$ and acetone-d_6, interaction energies (ΔE_{int}) calculated at PBE0-D3/def2-TZVP level of theory, and crystal structure XB parameters.

Code	NISac-**Z** (**Z** = **1**-**27**)				Code	NBSac-**Z** (**Z** = **1**-**27**)		
	$CDCl_3$ [M^{-1}]	**Acetone-d_6** [M^{-1}]	**I···O (Å)** [R_{XB}][a] ***d(NO)* (Å); ∠(NIO) (°)**	**ΔE_{int}** [kJ mol^{-1}]		**$CDCl_3$** [M^{-1}]	**Br···O (Å)** [R_{XB}][a] ***d(NO)* (Å), ∠(NIO) (°)**	**ΔE_{int}** [kJ mol^{-1}]
NISac-**1**[b]	3121±417	435±33	2.328(8) [0.665] 4.466(11);177.2(3)	–70.2	NBSac-**1**	24±1	*	–47.5
NISac-**2**[b]	16337±6317	2774±70	2.316(3) [0.662] 4.449(5);178.08(10)	–75.6	NBSac-**2**	33±1	2.275(2) [0.675] 4.192(3); 178.04(7)	–51.1
NISac-**3**[c]	6387±784	2276±125	2.302(3) [0.658] 4.447(5); 179.37(12)	–73.6	NBSac-**3**	28±1	2.327(2) [0.691] 4.235(4); 178.0(1)	–51.2
NISac-**4**	2543±220	5868±397	2.298(3) [0.657] 4.436(5); 177.66(14)	–76.6	NBSac-**4**	69±2	2.256(5) [0.669] 4.180(6); 177.88(16)	–52.2
NISac-**5**	3300±352	703±74	2.276(2) [0.650] 4.454(3); 176.14(10)	–80.5	NBSac-**5**[d]	41±1	2.402(2) [0.713] 4.281(3); 176.15(11)	–55.7
NISac-**6**	3410±518	19050±2222	2.321(7) [0.663] 4.476(9); 176.9(2)	–82.0	NBSac-**6**	90±2	*	–56.2
NISac-**7**	>10^8[e]	2899±332	*	–86.5	NBSac-**7**	353±38	2.268(4) [0.673] 4.194(5); 178.36(17)	–60.5
NISac-**8**	26224±13367	5475±349	*	–91.9	NBSac-**8**	36±2	*	–65.7
NISac-**9**	13431±1401	2625±201	2.315(2) [0.661] 4.448(3); 174.72(7)	–82.8	NBSac-**9**	21±1	*	–59.7
NISac-**10**	1238±138	4932±1508	2.295(7) [0.656] 4.442(14); 179.2(3)	–85.7	NBSac-**10**	163±6	*	–60.0
NISac-**11**	7244±1931	**	*	–79.8	NBSac-**11**	31±2	*	–55.6
NISac-**12**	1180±140	**	*	–110.1	NBSac-**12**	10±1	*	–81.5
NISac-**13**	**	**	*	–120.3	NBSac-**13**	66±3	*	–81.0
NISac-**14**	57650±21948	1288±27	*	–84.3	NBSac-**14**	19±1	2.303(2) [0.684] 4.210(3); 175.12(9)	–58.2
NISac-**15**	38841±22309	1466±54	2.341(4) [0.669] 4.479(5); 175.97(15)	–84.1	NBSac-**15**	13±1	*	–59.5
NISac-**16**[b]	14200±3034	2098±63	2.315(5) [0.661] 4.456(5);176.86(13)	–74.0	NBSac-**16**	24±1	2.337(3) [0.693] 4.250(7); 177.65(10)	–50.0
NISac-**17**[d]	203282[e]	304±5	2.436(3) [0.696] 4.534(5); 179.38(14)	–91.1	NBSac-**17**	8±1	*	–64.2
NISac-**18**	7668±820	942±19	*	–87.5	NBSac-**18**	28±1	*	–60.5
NISac-**19**	342689[e]	474±9	*	–93.4	NBSac-**19**	3±1	*	–65.7
NISac-**20**	**	7665±907	2.286(2) [0.653] 4.434(2); 177.31(5)	–79.2	NBSac-**20**	115±1	2.217(2) [0.658] 4.163(3); 177.75(8)	–54.1
NISac-**21**	79984±1688	3812±619	*	–90.6	NBSac-**21**	377±10	2.269(9) [0.673] 4.186(14); 178.8(4)	–63.7
NISac-**22**	17861±1963	91453±30334	2.326(6) [0.664] 4.455(4); 178.39(9)	–77.4	NBSac-**22**[c]	76±1	2.262(2) [0.671] 4.181(4); 179.17(8)	–52.9
NISac-**23**	4210±493	6282±224	*	–78.3	NBSac-**23**	69±1	2.232(3) [0.662] 4.166(4); 177.37(10)	–52.2
NISac-**24**	46196±13357	2221±201	*	–85.9	NBSac-**24**	42±1	*	–61.0
NISac-**25**	24361±3162	3711±311	2.343(3) [0.669] 4.474(4); 176.48(11)	–77.0	NBSac-**25**	47±1	2.298(2) [0.682] 4.211(2); 175.97(6)	–52.3
NISac-**26**	69040[e]	1072±14	*	–86.3	NBSac-**26**	20±3	*	–58.7
NISac-**27**	223821[e]	2656±67	*	–78.1	NBSac-**27**	52±1	2.297(2) [0.682] 4.202(3); 175.88(9)	–53.6

[a]The R_{XB}, is defined as [$R_{XB} = d_{XB}/(X_{vdw}+B_{vdw})$], where d_{XB} [Å] is the distance between donor (X) and the acceptor atoms (B), X_{vdw} and B_{vdw} are vdW radii [Å] of the corresponding atoms; The vdW radii determined by Bondi were used to calculate R_{XB} values[88]; [b]Results from previous report[72]; [c]In asymmetric units with Z'>1, R_{XB} value is calculated only for the shortest X···O distance; [d]*N*–Oxide oxygen is bidentate acceptor, and R_{XB} value is calculated only for the shortest X···O distance; [e]The K_{XB} contain excessive error and is unreliable, and presented only for reference purpose; *Crystal structure not available; **K_{XB} estimation unsuccessful due to ^{1}H NMR signal broadening.

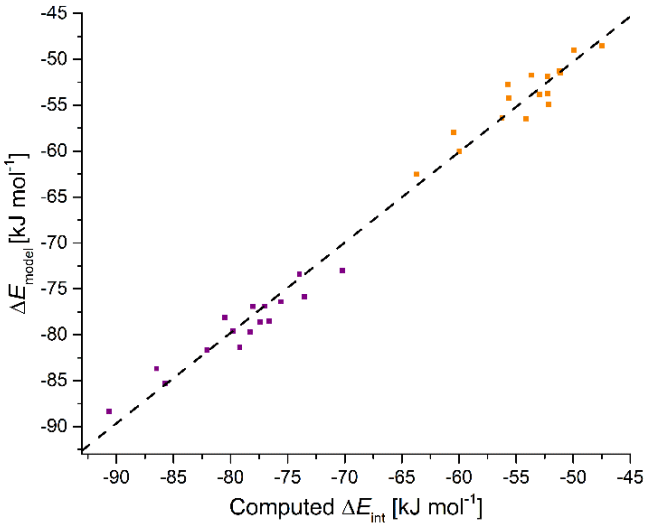

Figure 4. Plot of XB interaction energy ΔE_{model} estimated by double regression analysis of $Q_{oxygen}\times V_{S,max}$ and $1/I_{S,min}$(oxygen) *vs* ΔE_{int} calculated at PBE0-D3/def2-TZVP level for 32 XB complexes. Color code: NISac-**Z** (purple) and NBSac-**Z** (orange). [ΔE_{model} = 0.95(±0.03)×($Q_{oxygen}\times V_{S,max}$)–1760(±190)× $1/I_{S,min}$(oxygen)+220(±30)].

Benefits of simplified electrostatic model (ΔE_{model})

The presented simplified model significantly reduced the computational time compared to full DFT calculations. For example, the geometry optimization of NISac and **19**, and the analysis of Q_{oxygen}, $V_{S,max}$ and $1/I_{S,min}$ to obtain energies using ΔE_{model} at PBE0-D3/def2-TZVP level requires only 11 hours and 17 minutes of CPU time. Whilst the optimization of NISac-**19** to determine ΔE_{int} consumes 142 hours and 9 minutes of CPU time when the tasks were performed using the same computer cluster.

In case of the ωB97X-D/aug-cc-pVTZ(PP) method, the corresponding CPU times for a medium-sized XB complex, *e.g*. NISac-**10,** are 22 hours 42 minutes (ΔE_{model}) and 1585 hours 15 minutes (full DFT) for NISac and **10**, and the NISac-**10** optimization, respectively, implying even higher computational time savings. It is worth noting that the calculated σ-hole strengths for unperturbed donors reported by Huber *et al*. failed to predict the trends of the XB strengths in $CX_3I\cdots Y$ (X = F, Cl, Br, I and Y = F^-, Cl^-, Br^-, I^-, NMe_2) complexes.[91] However, later, it was shown that correct trends of I···Y XB strengths can be predicted if the polarization of donor halogen in the presence of the acceptor is described.[92] The accurate prediction of $N{-}X\cdots{}^-O{-}N^+$ interaction strengths by ΔE_{model} here, suggest that inclusion of σ-hole parameters to molecular mechanics (MM) force fields to model the influence the anisotropy of donor atom electrostatic surface potentials have on XBs could result in better descriptions of halogen-bonded systems by MM.[93–96]

Solution Studies

^{1}H NMR Association Constants

The association constants (K_{XB}) were determined by ^{1}H NMR titrations in $CDCl_3$ or acetone-d_6 at 298.0 K. The chemical shift changes of the donor protons were used as evidence for XB complexation in solution. As an example, the NISac-**4** binding curve obtained by non-linear least squares fitting using the program, HypNMR2008,[97] is shown in Fig.5. [For details, See Chapter S3 in the SI]. High binding constants of NISac-**Z** complexes in $CDCl_3$ resulted in large fitting errors, therefore to minimize the fitting errors between the calculated and observed binding curves, titrations were carried out up to 24 data points. For reference purposes, the ^{1}H NMR titrations were also carried out in XB competing solvent, acetone-d_6. The concentration dependence of ^{1}H NMR chemical shifts were measured for three selected NISac-**Z** complexes, and found to be very small (SI, Fig. S174 – S176).

Correlations between gas-phase ΔE_{int} and experimental Gibbs free energies derived from association constants have been reported in the literature.[21,23] In this work, the XB complexation enthalpies $\Delta H^{PCM}_{complex}$ calculated using polarized continuum model (PCM) for chloroform and ^{1}H NMR pK_{XB} values for 30 complexes,[99] correlate linearly with R^2 = 0.832 for both NBSac-**Z** and NISac-**Z** complexes [Fig. 6a]. Some NISac-**Z** complexes deviate from linearity which can be justified given the high fitting errors in ^{1}H NMR pK_{XB} values. The good performance of the simplified electrostatic model in predicting XB interaction energies prompted us to test the correlation between ΔE_{model} and experimental pK_{XB} values [Fig. 6b]. This resulted in correlation of R^2 = 0.826, which is close to that found for $\Delta H^{PCM}_{complex}$ vs pK_{XB}. This suggests that the electrostatic/polarization model can give good estimates of relative stabilities of XB complexes even in solution, if non-competitive solvents like $CDCl_3$ are used. In contrast, if XB complexes with additional interactions in their optimized structures are included in the $\Delta H^{PCM}_{complex}$ vs pK_{XB} correlation it becomes much worse (R^2 = 0.664) [SI, Fig. S14]. This hints that in solution, the additional H-bonding interactions at the *N*-oxide group orthogonal to the XB can affect the nucleophilicity of the O-atom and consequently lead in most cases to weaker association constants compared to the expected values based on calculated complexation enthalpies. Of the NISac-**Z** complexes included in the fit, the largest disagreement between the calculated $\Delta H^{PCM}_{complex}$ and experimental pK_{XB} values was found for NISac-**10**. The smaller than expected pK_{XB} value here can be rationalized by the competitive interference of water content of NMR solvents and the use of titrant **10** in its purchased form, $C_6H_7NO_2.xH_2O$.

10.1002/anie.201909759

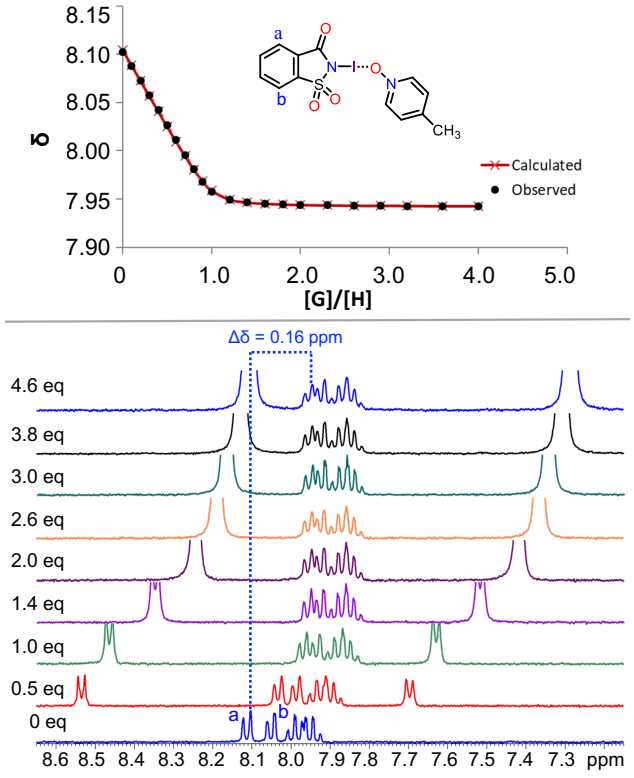

Figure 5. The fitting curves between observed and calculated chemical shifts followed by ^{1}H NMR titration spectral changes of NISac with the addition of **4**.

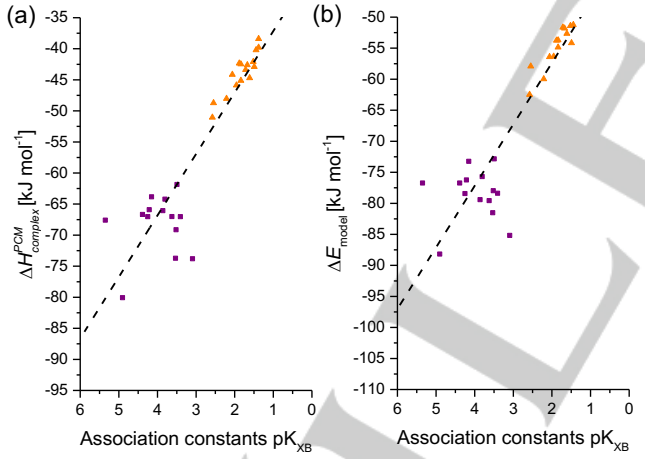

Figure 6. Correlation plots of, (a) XB complexation enthalpies in chloroform calculated by using PCM model $\Delta H^{PCM}_{complex}$ (R^2 = 0.832) and, (b) XB interaction energies calculated by using simplified electrostatic model ΔH^{PCM}_{model} (R^2 = 0.826) with pK$_{XB}$ derived from ^{1}H NMR titration experiments for NISac-**Z** (purple squares) and NBSac-**Z** (orange triangles) complexes.

^{1}H, ^{15}N-HMBC NMR Studies

The ^{1}H, ^{15}N-HMBC studies involve measurement of ^{15}N chemical shift of free ligands ($\delta^{15}N_{ligand}$) and complexes ($\delta^{15}N_{complex}$), and the coordination chemical shift, $\delta^{15}N_{coord}$, defined as $\delta^{15}N_{complex}$ - $\delta^{15}N_{ligand}$ is used to assess the XB complexation in N-heterocycles.[70,100] The ^{15}N shifts were measured for free acceptors **1**–**27**, and for the N-atom of the *N*-oxide group involved in N−X···$^{-}$O−N^{+} halogen bond. Due to the absence of hydrogen at 3-position to the donor N-atom, it is not possible to obtain the $\delta^{15}N_{coord}$ for *N*-halosaccharins, therefore only one δ^{15}N signal could be observed for each XB complex [For more details, See chapter S3 in the SI]. Upon N−X···$^{-}$O−N^{+} halogen bond formation, the N-atom of $^{-}$O−N^{+} group in NISac-**Z** complexes ($\delta^{15}N_{coord}$ range, 8.2 to 20.2 ppm) experiences larger ^{15}N chemical shift changes compared to NBSac-**Z** ($\delta^{15}N_{coord}$ range, 2.3 to 13.5 ppm), with the exception for NBSac-**13** ($\delta^{15}N_{coord}$, 22.2 ppm). The difference in $\delta^{15}N_{coord}$ chemical shifts for $^{-}$O−N^{+} groups, as a qualitative assessment, reflects the strong N−I···$^{-}$O−N^{+} and weak N−Br···$^{-}$O−N^{+} interactions. The $\delta^{15}N_{coord}$ chemical shifts of the N−X···$^{-}$O−N^{+} XBs range from 2.3 to 22.3 ppm and are, 45 to 5 times smaller than the $\delta^{15}N_{coord}$ values (≥100 ppm) found in pyridine-based [N–X–N]$^{+}$ complexes,[67,70,71] and one to three times larger than those observed for weak C−X···N (X = Br, I; $\delta^{15}N_{coord}$ range, 2.0 to 8.0 ppm) XB interactions.[101] The significantly larger $\delta^{15}N_{coord}$ values for [N–X–N]$^{+}$ are due to the direct participation of the N-atoms in the XB coordination and the effective positive charge delocalization over a 3*c*4*e* [N–X–N]$^{+}$ halogen-bonded system.[67,70,71] In N−X···$^{-}$O−N^{+} XBs, the atoms of $^{-}$O−N^{+} groups of *N*-oxides can be considered to be formally charged. The strong X^{+}···$^{-}$O interaction commences mostly through the interaction of oxygen electron density with the halogen atom without the direct involvement of the N-atom [Fig.7]. Thus, the $\delta^{15}N_{coord}$ values in N−X···$^{-}$O−N^{+} XBs can be expected to be smaller.

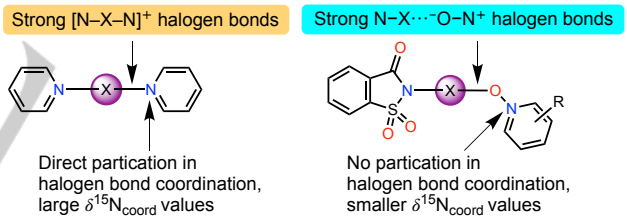

Figure 7. Pictorial representation comparing $\delta^{15}N_{coord}$ shifts in (left-side). [N–X–N]$^{+}$, and (right-side) N−X···$^{-}$O−N^{+} XBs.

X-Ray crystallography

Monodentate,[45,59] μ$_2$-*O*,*O* bidentate[61] and μ$_3$-*O*,*O*,*O* tridentate[55] XB modes of *N*-oxides are reported in the literature. Here, out of 27 X-ray crystal structures, only NISac-**17** and NBSac-**5** crystallizes in 2:1 donor:acceptor ratio, where the *N*-oxide oxygen functions in a bidentate XB acceptor mode [e.g. Fig. 8b]. The μ$_2$-*O*,*O* X···O bond distances in NISac-**17** and NBSac-**5** differ by *ca*. 0.108 Å and 0.025 Å, respectively. The R_{XB} value in NBSac-**5** is close to R_{HB} value of H-Bond complex, NSacH-**5** [Fig. 8f. For more R_{XB} and R_{HB} comparisons, see Table S13]. In NISac-**3** and NBSac-**22**, the asymmetric units contain more than one 1:1 donor:acceptor complex ($Z' > 1$), each 1:1 donor:acceptor complex show different X···O bond distances. Out of the complexes studied here, the shortest X···O distances are manifested by NISac-**5** [R_{XB} = 0.650] in the NISac-**Z** series, and NBSac-**20** [R_{XB} = 0.658] in the NBSac-**Z** series.

10.1002/anie.201909759

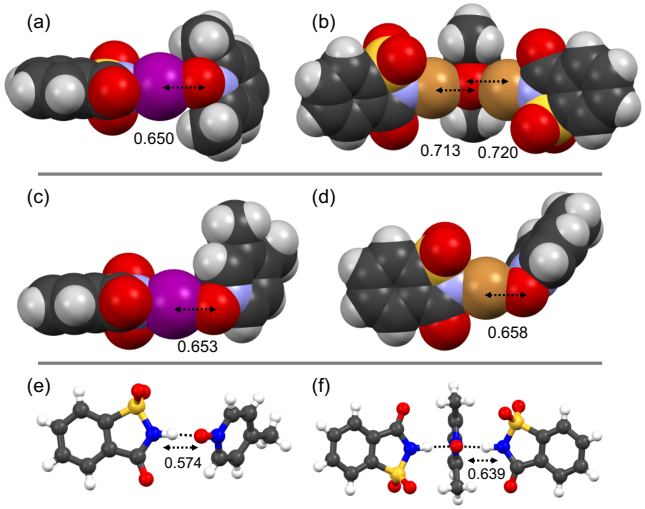

Figure 8. X-Ray crystal structure of (a) NISac-**5**, (b) NBSac-**5**, (c) NISac-**20** and (d) NBSac-**20** in CPK models, and HB complexes (e) NSacH-**4**, and (f) NSacH-**5** in ball and stick model. The value below double-headed arrow is R_{XB} and R_{HB}. Note: The N–H distances were normalized to 1.0 Å.

The donor N−X bond lengths in the crystal structures of *N*-oxide complexes are less affected by the electron density of the *N*-oxide oxygen than they are by the N-atom of the pyridine in the N-halosaccharin-pyridine complexes reported by Fourmigue *et al*.[43] For example, the complexed donor N−I and N−Br bond lengths in NISac-**5** and NBSac-**20** are shorter by *ca*. 0.112 Å and 0.126 Å, respectively, than in N-halosaccharin-pyridine complexes, NISac-N_{Py1}[43] and NBSac-N_{Py2},[101] by Fourmigue *et al*. (**Py1** = DMAP, **Py2** = 4-methylpyridine) [See Table 2]. The extremely short N−X···N distances for N-halosaccharin-pyridine systems, and their remarkable structural similarity with $[N–X–N]^+$ complexes, is due to the efficient overlap of pyridine N-atom lone-pair and *p*-orbital of the donor halogen. The magnitude of overlapping is often enhanced by, electron donating substituents appended to the acceptor pyridines, and π-delocalization across the (coplanar) donor-acceptor molecules,[71] a feature that is not available in N−X···$^-$O−N^+ XBs [Fig. 3 and Fig. 7]. The (imide)N···O(PyNO) distances, on the other hand, vary within a narrow range, 4.434(2) – 4.481(2) Å for NISac-**Z,** and 4.163(2) – 4.250(4) Å for NBSac-**Z** complexes, implying that only the donor halogen position is altered between N- and O-atoms. The (imide)N···O(PyNO) distances of, NISac-**Z** are *ca*. ~0.100 Å shorter than (imide)N···N(**py**) of NISac-N_{py}[43,44,87] and, NBSac-**Z** are *ca*. ~0.07 Å shorter when compared to (imide)N···N(**py**) of NBSac-N_{py} complexes.[43,44,87] These findings suggest that the donor halogens of N-halosaccharins are highly sensitive towards the electron density of the acceptor atoms, which is evidently larger for O-atom of aromatic *N*-oxides. Yet, surprisingly the *N*-atom of parent N-aromatics NI/BSac-N_{py} forms very strong XBs. Nevertheless, the narrow range (imide)N···O(PyNO) distance variations in studied N−X···$^-$O−N^+ XBs when compared to the range N···N distances in 3*c*4*e* $[N–X–N]^+$ complexes [see Table S1] is a good qualitative indication that the N−X···$^-$O−N^+ XBs manifest exceptionally strong electrostatic interactions between the X- and O-atom. How the calculated XB interaction energies from crystal structures (ΔE_{int}^{cryst}) correlate with the ΔE_{int}^{opt} is shown in SI (Chapter 4.3.2).

Table 2. Experimental solid-state data comparison of XB parameters

Complex	N–I (Å) in NISac[a]	N–I (Å) in XB complex	I···O/N (Å)	R_{XB}
NISac-**5**	2.020 [b]	2.180(3)	2.276(2)	0.650
NISac-N_{Py1}		2.292(2)[c]	2.218(2)	0.631
$[N–I–N]^+$	--	2.257(7) [d]	--	0.639
Complex	**N–Br (Å) in NBSac[a]**	**N–Br (Å) in XB complex**	**Br···O/N (Å)**	**R_{XB}**
NBSac-**20**	1.827(4)[e]	1.947(2)	2.217(2)	0.658
NBSac-N_{Py2}		2.073(6) [f]	2.098(6)	0.617
$[N–Br–N]^+$	--	2.092(2) [g]	--	0.598

[a]N–X Bond distances in uncomplexed donor; [b]Optimized structure (See Table S3); CCDC Nos: [c]OGIWUY; [d]HUMMAD02; [e]MUGDOI; [f]KECJAG; [g]DOWBAU; **Py1** = DMAP; **Py2** = 4-methylpyridine.

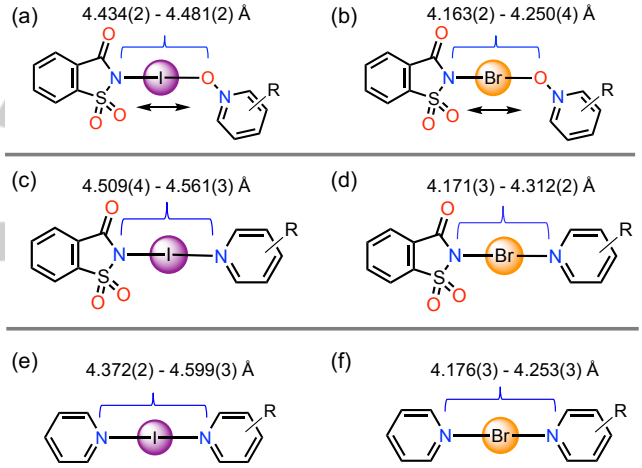

Figure 9. Comparison of (a & b) (imide)N···O(PyNO) distances of N−X···$^-$O−N^+ XBs to N···N distances in (c & d) N-halosaccharin-pyridine, and (e & f) 3*c*4*e* $[N–X–N]^+$complexes.

Conclusion

Strong N−X···$^-$O−N^+ (X = I, Br) XBs using N-I/BSac as the donor and *N*-oxide oxygen as the acceptor come close to the strength of the $[N–X–N]^+$ XBs. The combined DFT computational-experimental study, performed on N-halosaccharins and pyridine *N*-oxides with -CH_3, -OCH_3, -Ph, -Et, -Bz and -iPr substituents, proved to be an effective method to understand the behaviour of the N−X···$^-$O−N^+ XBs. Using a simplified electrostatic/polarization model the strengths of the N−X···$^-$O−N^+ XBs could be predicted with good accuracy when compared to XB strengths and geometries from ^{1}H NMR and X-ray crystallography experiments. The N−X···$^-$O−N^+ XBs in this study were found to be strong (-47.5 to –120.3 kJ mol^{-1}) but weaker than the very strong $[N–X–N]^+$ XBs (~160 kJ mol^{-1}). The exceptional XB strength for the 3*c*4*e* $[N–X–N]^+$ complexes originates from the direct XB coordination to the pyridine N-atom, that is part of the π-system. Such coordination facilitates the donor-acceptor systems not only a tight overlapping between pyridine N-atom lone pair and halogen σ-hole, but also

π-electron delocalization across (aromatic)N···X···N(aromatic) bonds. This feature is not available in aromatic *N*-oxides, where the O-atom is not a part of the π-system and therefore the shortening of the X···O halogen bonds in N−X···$^{-}$O−N^{+} reflects the strong electrostatic attractions between large electron density on *N*-oxide O-atom and halogen σ-hole.

For N−I···$^{-}$O−N^{+} XBs, the association constants (K_{XB}) in $CDCl_3$ range from 1180 to >10^8 M^{-1}. Yet, the N−I bond lengths in X-ray crystal structures are not significantly affected by the electron density of the *N*-oxide oxygen. The N−I bond distances in XB complexes increase maximum ~0.160 Å, while the (imide)N···O(PyNO) distances vary only 0.047 Å. Thus correlating the X-ray based X···O bond distances and the ^{1}H NMR binding constants can lead to errors, as X···O bond distances in solid-state are very similar while the corresponding association constants can be very different. This suggests that the short N−X···$^{-}$O−N^{+} distances in crystal structures result in from locally maximized lattice interactions and do not reflect the intrinsic XB strengths.

Acknowledgements

The authors gratefully acknowledge financial support from the Academy of Finland (RP grant no. 298817), grants of computational resources from the Finnish Grid and Cloud Infrastructure (urn:nbn:fi:research-infras-2016072533) and CSC – IT Center for Science, and the University of Jyväskylä. The help of Prof. Dr. Christoph Schalley and M.Sc. Henrik Hupatz (Freie Universität Berlin, Germany), Dr. Alexander S. Novikov with the computational studies (Saint Petersburg State University, Russia), and Prof. Dr. Heikki Tuononen (University of Jyväskylä, Finland) for valuable suggestions for the 1st version of the manuscript are gratefully acknowledged.

Keywords: Halogen bond • *N*-oxide • N-Haloimide • Saccharin • Sigma hole

[1] G. R. Desiraju, P. S. Ho, L. Kloo, A. C. Legon, R. Marquardt, P. Metrangolo, P. Politzer, G. Resnati and K. Rissanen, *Pure Appl. Chem.* **2013**, *85*, 1711.

[2] G. Cavallo, P. Metrangolo, R. Milani, T. Pilati, A. Priimagi, G. Resnati, G. Terraneo, *Chem. Rev.* **2016**, *116*, 2478–2601.

[3] L. Carreras, M. Serrano-Torné, P. W. N. M. van Leeuwen, A. Vidal-Ferran, *Chem. Sci.* **2018**, *9*, 3644–3648.

[4] D. Bulfield, S. M. Huber, *Chem. – A Eur. J.* **2016**, *22*, 14434–14450.

[5] M. Breugst, D. von der Heiden, J. Schmauck, *Synthesis (Stuttg).* **2017**, *49*, 3224–3236.

[6] J. Y. C. Lim, P. D. Beer, *Chem* **2018**, *4*, 731–783.

[7] I. Piquero-Zulaica, J. Lobo-Checa, A. Sadeghi, Z. M. A. El-Fattah, C. Mitsui, T. Okamoto, R. Pawlak, T. Meier, A. Arnau, J. E. Ortega, et al., *Nat. Commun.* **2017**, *8*, 787.

[8] L. Xing, W. Jiang, Z. Huang, J. Liu, H. Song, W. Zhao, J. Dai, H. Zhu, Z. Wang, P. S. Weiss, et al., *Chem. Mater.* **2019**, *31*, 3041–3048.

[9] L. González, N. Gimeno, R. M. Tejedor, V. Polo, M. B. Ros, S. Uriel, J. L. Serrano, *Chem. Mater.* **2013**, *25*, 4503–4510.

[10] M. Meyns, F. Iacono, C. Palencia, J. Geweke, M. D. Coderch, U. E. A. Fittschen, J. M. Gallego, R. Otero, B. H. Juárez, C. Klinke, *Chem. Mater.* **2014**, *26*, 1813–1821.

[11] M.-P. Zhuo, J.-J. Wu, X.-D. Wang, Y.-C. Tao, Y. Yuan, L.-S. Liao, *Nat. Commun.* **2019**, *10*, 3839.

[12] O. Bolton, K. Lee, H.-J. Kim, K. Y. Lin, J. Kim, *Nat. Chem.* **2011**, *3*, 205–210.

[13] L. González, R. M. Tejedor, E. Royo, B. Gaspar, J. Munárriz, A. Chanthapally, J. L. Serrano, J. J. Vittal, S. Uriel, *Cryst. Growth Des.* **2017**, *17*, 6212–6223.

[14] D. W. Bruce, P. Metrangolo, F. Meyer, T. Pilati, C. Präsang, G. Resnati, G. Terraneo, S. G. Wainwright, A. C. Whitwood, *Chem. – A Eur. J.* **2010**, *16*, 9511–9524.

[15] X. Tong, Y. Qiu, X. Zhao, B. Xiong, R. Liao, H. Peng, Y. Liao, X. Xie, *Soft Matter* **2019**, *15*, 6411–6417.

[16] L. Meazza, J. A. Foster, K. Fucke, P. Metrangolo, G. Resnati, J. W. Steed, *Nat Chem* **2013**, *5*, 42–47.

[17] S. Bhattacharjee, S. Bhattacharya, *Langmuir* **2016**, *32*, 4270–4277.

[18] P. Metrangolo, G. Resnati, H. D. Arman, *Halogen Bonding: Fundamentals and Applications*, Springer, **2008**.

[19] T. Brinck, A. N. Borrfors, *J. Mol. Model.* **2019**, *25*, 125.

[20] C. B. Aakeröy, A. S. Sinha, *Co-Crystals: Preparation, Characterization and Applications*, Royal Society Of Chemistry, **2018**.

[21] M. G. Sarwar, B. Dragisic, L. J. Salsberg, C. Gouliaras, M. S. Taylor, *J. Am. Chem. Soc.* **2010**, *132*, 1646–1653.

[22] S. H. Jungbauer, D. Bulfield, F. Kniep, C. W. Lehmann, E. Herdtweck, S. M. Huber, *J. Am. Chem. Soc.* **2014**, *136*, 16740–16743.

[23] M. G. Chudzinski, M. S. Taylor, *J. Org. Chem.* **2012**, *77*, 3483–3491.

[24] R. Cabot, C. A. Hunter, *Chem. Commun.* **2009**, 2005–2007.

[25] A. Bauzá, A. Frontera, *Phys. Chem. Chem. Phys.* **2017**, *19*, 12936–12941.

[26] C. B. Aakeröy, M. Baldrighi, J. Desper, P. Metrangolo, G. Resnati, *Chem. – A Eur. J.* **2013**, *19*, 16240–16247.

[27] S. T. Nguyen, T. L. Ellington, K. E. Allen, J. D. Gorden, A. L. Rheingold, G. S. Tschumper, N. I. Hammer, D. L. Watkins, *Cryst. Growth Des.* **2018**, *18*, 3244–3254.

[28] C. B. Aakeröy, T. K. Wijethunga, J. Desper, M. Đaković, *Cryst. Growth Des.* **2015**, *15*, 3853–3861.

[29] S. T. Nguyen, A. L. Rheingold, G. S. Tschumper, D. L. Watkins, *Cryst. Growth Des.* **2016**, *16*, 6648–6653.

[30] V. Stilinović, G. Horvat, T. Hrenar, V. Nemec, D. Cinčić, *Chem. – A Eur. J.* **2017**, *23*, 5244–5257.

[31] O. Dumele, D. Wu, N. Trapp, N. Goroff, F. Diederich, *Org. Lett.* **2014**, *16*, 4722–4725.

[32] L. C. F. Morgan, Y. Kim, J. N. Blandy, C. A. Murray, K. E. Christensen, A. L. Thompson, *Chem. Commun.* **2018**, *54*, 9849–9852.

[33] A. A. Neverov, H. X. Feng, K. Hamilton, R. S. Brown, *J. Org. Chem.* **2003**, *68*, 3802–3810.

[34] C. Álvarez-Rúa, S. García-Granda, A. Ballesteros, F. González-Bobes, J. M. González, *Acta Crystallogr. Sect. E* **2002**, *58*, o1381--o1383.

[35] Y.-M. Wang, J. Wu, C. Hoong, V. Rauniyar, F. D. Toste, *J. Am. Chem. Soc.* **2012**, *134*, 12928–12931.

[36] M.-J. Crawford, M. Göbel, K. Karaghiosoff, T. M. Klapötke, J. M. Welch, *Inorg. Chem.* **2009**, *48*, 9983–9985.

[37] J. Grebe, G. Geiseler, K. Harms, B. Neumüller, K. Dehnicke, *Angew. Chemie Int. Ed.* **1999**, *38*, 222–225.

[38] C. Weinberger, R. Hines, M. Zeller, S. V Rosokha, *Chem. Commun.* **2018**, *54*, 8060–8063.

[39] H. Pritzkow, *Acta Crystallogr. Sect. B* **1975**, *31*, 1505–1506.

[40] C. P. Brock, Y. Fu, L. K. Blair, P. Chen, M. Lovell, *Acta Crystallogr. Sect. C* **1988**, *44*, 1582–1585.

[41] K. Raatikainen, K. Rissanen, *Chem. Sci.* **2012**, *3*, 1235–1239.

[42] K. Raatikainen, K. Rissanen, *CrystEngComm* **2011**, *13*, 6972–6977.

[43] O. Makhotkina, J. Lieffrig, O. Jeannin, M. Fourmigué, E. Aubert, E. Espinosa, *Cryst. Growth Des.* **2015**, *15*, 3464–3473.

[44] E. Aubert, E. Espinosa, I. Nicolas, O. Jeannin, M. Fourmigué, *Faraday Discuss.* **2017**, *203*, 389–406.

[45] G. R. Hanson, P. Jensen, J. McMurtrie, L. Rintoul, A. S. Micallef, *Chem. – A Eur. J.* **2009**, *15*, 4156–4164.

[46] Y. P. Nizhnik, A. Sons, M. Zeller, S. V Rosokha, *Cryst. Growth Des.* **2018**,

18, 1198–1207.

[47] M. R. Scholfield, C. M. Vander Zanden, M. Carter, P. S. Ho, *Protein Sci.* **2013**, *22*, 139–152.

[48] W. X. Wu, M. Liu, H. Wang, W. J. Jin, *Cryst. Growth Des.* **2019**, *19*, 4378–4384.

[49] P. A. Raffo, F. D. Cukiernik, R. F. Baggio, *Acta Crystallogr. Sect. C* **2015**, *71*, 84–88.

[50] C. B. Aakeröy, P. D. Chopade, J. Desper, *Cryst. Growth Des.* **2013**, *13*, 4145–4150.

[51] R. Liu, H. Wang, W. J. Jin, *Cryst. Growth Des.* **2017**, *17*, 3331–3337.

[52] W. X. Wu, H. Wang, W. J. Jin, *Cryst. Growth Des.* **2018**, *18*, 6742–6747.

[53] M. T. Messina, P. Metrangolo, W. Panzeri, T. Pilati, G. Resnati, *Tetrahedron* **2001**, *57*, 8543–8550.

[54] R. Puttreddy, F. Topić, A. Valkonen, K. Rissanen, *Crystals* **2017**, *7*, 214.

[55] F. Topić, R. Puttreddy, J. M. Rautiainen, H. M. Tuononen, K. Rissanen, *CrystEngComm* **2017**, *19*, 4960–4963.

[56] B. Galmés, A. Franconetti, A. Frontera, *Int. J. Mol. Sci.* **2019**, *20*, 3440.

[57] C. Cavallotti, P. Metrangolo, F. Meyer, F. Recupero, G. Resnati, *J. Phys. Chem. A* **2008**, *112*, 9911–9918.

[58] W. Borley, B. Watson, Y. P. Nizhnik, M. Zeller, S. V Rosokha, *J. Phys. Chem. A* **2019**, *123*, 7113–7123.

[59] K. Boubekeur, J.-L. Syssa-Magalé, P. Palvadeau, B. Schöllhorn, *Tetrahedron Lett.* **2006**, *47*, 1249–1252.

[60] V. Mugnaini, C. Punta, R. Liantonio, P. Metrangolo, F. Recupero, G. Resnati, G. F. Pedulli, M. Lucarini, *Tetrahedron Lett.* **2006**, *47*, 3265–3269.

[61] C. B. Aakeröy, T. K. Wijethunga, J. Desper, *CrystEngComm* **2014**, *16*, 28–31.

[62] L. Turunen, U. Warzok, C. A. Schalley, K. Rissanen, *Chem* **2017**, *3*, 861–869.

[63] L. Turunen, U. Warzok, R. Puttreddy, N. K. Beyeh, C. A. Schalley, K. Rissanen, *Angew. Chemie - Int. Ed.* **2016**, *55*, 14033–14036.

[64] L. Turunen, A. Peuronen, S. Forsblom, E. Kalenius, M. Lahtinen, K. Rissanen, *Chem. - A Eur. J.* **2017**, *23*, 11714–11718.

[65] A.-C. C. Carlsson, J. Gräfenstein, J. L. Laurila, J. Bergquist, M. Erdélyi, *Chem. Commun.* **2012**, *48*, 1458–1460.

[66] S. B. Hakkert, M. Erdélyi, *J. Phys. Org. Chem.* **2015**, *28*, 226–233.

[67] S. Lindblad, K. Mehmeti, A. X. Veiga, B. Nekoueishahraki, J. Gräfenstein, M. Erdélyi, *J. Am. Chem. Soc.* **2018**, *140*, 13503–13513.

[68] A. Karim, M. Reitti, A.-C. C. Carlsson, J. Gräfenstein, M. Erdélyi, *Chem. Sci.* **2014**, *5*, 3226–3233.

[69] M. Bedin, A. Karim, M. Reitti, A.-C. C. Carlsson, F. Topic, M. Cetina, F. Pan, V. Havel, F. Al-Ameri, V. Sindelar, K. Rissanen, J. Gräfenstein, M. Erdélyi, *Chem. Sci.* **2015**, *6*, 3746–3756.

[70] A.-C. C. Carlsson, K. Mehmeti, M. Uhrbom, A. Karim, M. Bedin, R. Puttreddy, R. Kleinmaier, A. A. Neverov, B. Nekoueishahraki, J. Gräfenstein, K. Rissanen, M. Erdélyi, *J. Am. Chem. Soc.* **2016**, *138*, 9853–9863.

[71] A.-C. C. C. Carlsson, J. Gräfenstein, A. Budnjo, J. L. Laurila, J. Bergquist, A. Karim, R. Kleinmaier, U. Brath, M. Erdélyi, *J. Am. Chem. Soc.* **2012**, *134*, 5706–5715.

[72] R. Puttreddy, O. Jurček, S. Bhowmik, T. Mäkelä, K. Rissanen, *Chem. Commun.* **2016**, *52*, 2338–2341.

[73] A. R. Katritzky, J. M. Lagowski, *Chemistry of the Heterocyclic N-Oxides*, Academic Press, **1971**.

[74] P. Politzer, J. S. Murray, T. Clark, *Phys. Chem. Chem. Phys.* **2010**, *12*, 7748–7757.

[75] P. Politzer, J. S. Murray, T. Clark, G. Resnati, *Phys. Chem. Chem. Phys.* **2017**, *19*, 32166–32178.

[76] T. Clark, P. Politzer, J. S. Murray, *Wiley Interdiscip. Rev. Comput. Mol. Sci.* **2015**, *5*, 169–177.

[77] J.-D. Chai, M. Head-Gordon, *Phys. Chem. Chem. Phys.* **2008**, *10*, 6615–6620.

[78] S. Kozuch, J. M. L. Martin, *J. Chem. Theory Comput.* **2013**, *9*, 1918–1931.

[79] J.-W. Zou, Y.-J. Jiang, M. Guo, G.-X. Hu, B. Zhang, H.-C. Liu, Q.-S. Yu, *Chem. – A Eur. J.* **2005**, *11*, 740–751.

[80] P. M. Morse, *Phys. Rev.* **1929**, *34*, 57–64.

[81] B. Nepal, S. Scheiner, *Phys. Chem. Chem. Phys.* **2016**, *18*, 18015–18023.

[82] A. Forni, *J. Phys. Chem. A* **2009**, *113*, 3403–3412.

[83] W. Zierkiewicz, D. C. Bieńko, D. Michalska, T. Zeegers-Huyskens, *Theor. Chem. Acc.* **2015**, *134*, 103.

[84] I. Alkorta, G. Sánchez-Sanz, J. Elguero, *CrystEngComm* **2013**, *15*, 3178–3186.

[85] P. Politzer, J. S. Murray, T. Clark, *Phys. Chem. Chem. Phys.* **2013**, *15*, 11178–11189.

[86] P. Politzer, J. S. Murray, *Theor. Chem. Acc.* **2012**, *131*, 1114:10.

[87] D. Dolenc, B. Modec, *New J. Chem.* **2009**, *33*, 2344–2349.

[88] A. Bondi, *J. Phys. Chem.* **1964**, *68*, 441–451.

[89] P. Sjoberg, J. S. Murray, T. Brinck, P. Politzer, *Can. J. Chem.* **1990**, *68*, 1440–1443.

[90] P. Politzer, J. S. Murray, F. A. Bulat, *J. Mol. Model.* **2010**, *16*, 1731–1742.

[91] S. M. Huber, E. Jimenez-Izal, J. M. Ugalde, I. Infante, *Chem. Commun.* **2012**, *48*, 7708–7710.

[92] T. Clark, A. Heßelmann, *Phys. Chem. Chem. Phys.* **2018**, *20*, 22849–22855.

[93] H. Torii, *J. Chem. Phys.* **2010**, *133*, 34504.

[94] M. Kolář, P. Hobza, *J. Chem. Theory Comput.* **2012**, *8*, 1325–1333.

[95] O. I. Titov, D. A. Shulga, V. A. Palyulin, N. S. Zefirov, *Dokl. Chem.* **2016**, *471*, 338–342.

[96] M. R. Scholfield, M. C. Ford, C. M. Vander Zanden, M. M. Billman, P. S. Ho, A. K. Rappé, *J. Phys. Chem. B* **2015**, *119*, 9140–9149.

[97] C. Frassineti, L. Alderighi, P. Gans, A. Sabatini, A. Vacca, S. Ghelli, *Anal. Bioanal. Chem.* **2003**, *376*, 1041–1052.

[98] T. M. Beale, M. G. Chudzinski, M. G. Sarwar, M. S. Taylor, *Chem. Soc. Rev.* **2013**, *42*, 1667–1680.

[99] NISac-**7** and NISac-**20** Structures were not included in the correlation plot, XB complexation enthalpies vs pKXB, due to the unsuccessful determination of NMR association constants.

[100] H. Andersson, A.-C. C. Carlsson, B. Nekoueishahraki, U. Brath, M. Erdélyi, Academic Press, **2015**, 73, pp. 73–210.

[101] S. B. Hakkert, J. Gräfenstein, M. Erdélyi, *Faraday Discuss.* **2017**, *203*, 333–346.

10.1002/anie.201909759

Entry for the Table of Contents

RESEARCH ARTICLE

Strong N–X···$^{-}$O–N^{+} (X = I, Br) halogen bonds, by using oxygen as halogen bond acceptor, are obtained from N-halosaccharins and aromatic *N*-oxides. The donor-acceptor dependent tunable X···O distances are investigated by using computational methods, solution NMR, and X-ray diffraction analysis.

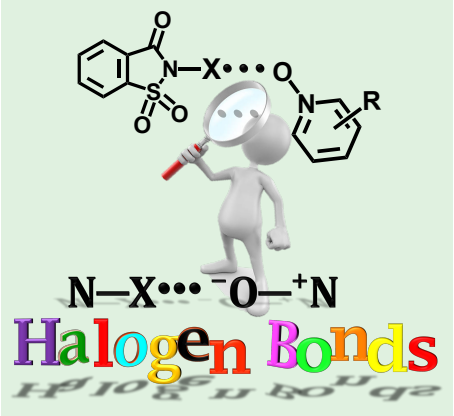

Rakesh Puttreddy, J. Mikko Rautiainen, Toni Mäkelä, Kari Rissanen**

Page No. – Page No.

Strong N–X···O–N Halogen Bonds: Comprehensive Study on N-Halosaccharin Pyridine *N*-oxide Complexes